Niger. J. Physiol. Sci. 39 (December 2024): 277 – 284
www.njps.physiologicalsociety.com

Niger. J. Physiol. Sci.

Full length Research Article

Changes in the Subcortical White Matter and the Pyramidal Neurons in the Sensorimotor Cortex of Juvenile Hydrocephalic Rats

Femi Akinlosotu O.M., *Olopade F.E., Okoye C.S. and Shokunbi M.T.

Developmental Neurobiology and Forensic Anatomy Unit, Department of Anatomy, College of Medicine, University of Ibadan, Ibadan, Nigeria

Summary: Hydrocephalus, the aberrant enlargement of the brain's ventricles, is caused by a build-up of cerebrospinal fluid that stretches the periventricular white matter and may disrupt the connections between the pyramidal neurons in the cerebral cortex. Using an intra-cisternal kaolin injection hydrocephalic rat model, we aimed to determine if the effects of hydrocephalus on the white matter will subsequently impact the dendrites of cortical pyramidal neurons, which are the synaptic sites for the white matter fibres, particularly the afferent fibres. Three-week-old hydrocephalic rats were compared with controls after 1 week, 2 weeks and 4 weeks. Dendritic arborisations of the pyramidal neurons were evaluated using a modified Golgi stain. Haematoxylin and Eosin, and Cresyl violet stains were used to measure cortical thickness and pyramidal neuronal count. The hydrocephalic rats' cerebral cortex and corpus callosum were thinner ($p<0.0001$) than the controls. Rats with hydrocephalus had a similar pyramidal neuron count to the controls, with no significant decline. After two weeks of hydrocephalic induction, the pyramidal neurons' dendritic branching changed due to basal dendritic reduction and denudation. Reduced thickness in the corpus callosum and sensorimotor cortex was observed in the hydrocephalus animals. The pyramidal cell population remained unaffected, but the basal dendrites of the cells were substantially weakened. Ventricular enlargements during the juvenile developmental stage may harm dendritic arborization, which could obstruct neurological maturation.

Keywords*: hydrocephalus, Golgi stain, pyramidal neurons, cortical thickness, corpus callosum, dendritic architecture*.

**Authors for correspondence: funmiolopade@yahoo.com , Tel: +234- 8052274102*

Manuscript received- September 2024; Accepted: November 2024

DOI: https://doi.org/10.54548/njps.v39i2.14

INTRODUCTION

Hydrocephalus is a neurological disorder classically considered a failure of cerebrospinal fluid (CSF) homeostasis from its point of production within the ventricular system to its point of absorption into the systemic circulation resulting in the active distension of the cerebral ventricles. This damage occurs in a multifactorial way, particularly as ventriculomegaly becomes more severe, with the prevalence of cortical thinning and distention, along with stretching of the septum pellucidum (Maller & Gray, 2016; Rekate & Blitz, 2016; Kahle *et al*., 2016, 2024). Neocortical pyramidal neurons are cerebral cortex's fundamental building blocks and the most prevalent type, with their soma located in layers V and VI. While the apical dendrites ascend towards the pia, basal dendrites fan out around the soma. During this process, they often give off oblique dendrites and end in a tuft of dendrites in layer 1 or other layers. Except for sporadic aberrant spines, both basal and apical dendrites normally have a high density of spines. A significant portion of the neocortex's output comes from these pyramidal neurons. Input signals from numerous brain regions' afferent fibers are combined, processed through several layers, and then transmitted to various locations via these pyramidal neurons. Excitatory synapses in the cortex are primarily derived from these cells, and the primary postsynaptic targets of excitatory synapses are their dendritic spines, or simply spines (Benavides-Piccione *et al*., 2021; Nolan *et al*., 2024). Their dendritic structures differ significantly between cortical areas, layers, and species. How they integrate information is greatly influenced by these variations in their neuronal architecture. They also contribute to almost all intra-areal, inter-areal, and subcortical projections, and they are the principal recipients of excitatory synapses (Chen *et al*., 2017; Galakhova *et al*., 2022; Hunt *et al*., 2023; Benavides-Piccione *et al*., 2024). Because of their greater size and complexity, dendritic trees offer greater computational diversity. Dendritic branches can function as distinct processing units on their own and perform discrete computations (Galakhova *et al*., 2022: Benavides-Piccione *et al*., 2024). Utilizing an intra-cisternal kaolin injection hydrocephalic rat model three weeks post-delivery and weaning, the present study is unique in that it measures the dendritic arborizations, cortical thickness and neuronal count of the pyramidal neurons in the cerebral

cortex. This study focuses on the pyramidal neurons of layer V of the cerebral cortex in young hydrocephalic rats to provide insight into the fate of their dendrites. We postulate that the impact of hydrocephalus on the white matter, which is composed of both afferent and efferent fibers, will subsequently influence the cerebral cortex's pyramidal neurons' dendrites, which serve as the sites of synapses for the white matter fibers, particularly the afferent fibers (Del Bigio, 2010; Chen *et al*., 2017; Curzio & Curzio, 2017).

MATERIALS AND METHODS

Animal Procurement, Care, and Management: All procedures on animal handling were conducted in compliance with the protocol of Institutional Animal Care and Use Committee of the National Institute of Health, USA, European Committee Council Directives (86/609/EEC) and ARRIVE guidelines, minimizing the number of animals used and avoiding their suffering. Fifteen sexually matured female and five male Wistar rats were procured from the Central Animal House of the Faculty of Basic Medical Sciences, University of Ibadan. They were mated in a 3:1 ratio of females to males per cage and housed in the Animal House of the Faculty of Basic Medical Science under normal temperature (32±2°C) and natural light/dark cycle conditions with ad libitum access to standard rat chow and water. Pregnant rats were housed separately until delivery and with their pups until the weaning period (postnatal day 21). At weaning, the pups were separated from the dams and hydrocephalus was induced.

Induction of hydrocephalus: Hydrocephalus was induced in the 3-week-old rats (26-28g) under ketamine/xylazine anaesthesia at 90/10mg/kg i.p. The cervical region of the rats was dapped with an ethanol-moistened cotton pad and flexed. The sub-occipital region for the rhomboid fossa marking the cisterna magna was detected by palpations with the index finger. Sterile kaolin suspension (0.02ml using 0.25g/ml in sterile water) was slowly injected into the cisterna magna using a 27-gauge needle. Post-injection, the rats were monitored for about 1hr after which they were returned to their cages. The control rats had a sham saline injection into the cisterna magna. This technique has previously been established in the literature as a viable way of inducing hydrocephalus in experimental animals (Olopade *et al*., 2021; Suryaningtyas *et al*., 2019).
Hydrocephalus was confirmed by the presence of a dome-shaped head (Chen *et al*., 2017; Suryaningtyas *et al*., 2019; Olopade *et al*., 2021). Body weights of rats were measured twice a week. The general behaviour of the rats and their head circumference were observed daily. Rats with marked rapid weight loss, unsteady gait, or fatigue were isolated from the litter to prevent attack from their mates.

Post-Induction Protocol: The rats were euthanized at one-week post induction; two weeks post induction and four weeks post induction respectively and grouped as such. Euthanasia commenced with ketamine/xylazine (90/10mg/kg) anaesthesia followed by trans cardiac perfusion with normal saline to flush off the blood and then with 10% neutral buffered formalin. The brains were quickly collected and fixed in 10% neutral buffered formalin for seven days. Coronal sections of the brains were made at the level of the optic chiasma and the diameter of the lateral ventricle at that level was measured in all the groups. Mild ventriculomegaly was defined as a ventricular diameter of less than 1.5mm, moderate ventriculomegaly as a ventricular diameter of more than 1.5mm with the cortex still opposed to the caudate/putamen and severe ventriculomegaly was defined as a visible separation of the cerebral cortex from the caudate/putamen with ventriculomegaly according to Olopade et. al. (2021).

Histological Studies: A subset of the brains in each group underwent the Golgi staining technique of Smith and Roopar 2012 (as described by Sarkala *et al*., 2023). The chromatin solution was prepared with 60 ml of 3% potassium dichromate solution and 20 ml of 10% formalin. The rat brains were transferred from the fixative into the chromatin solution and left in a dark place for two days. A second chromatin solution containing 60ml of 3g of potassium dichromate, 2 grams of chloral hydrate, and 5-7 drops of Dimethyl sulphoxide mixed in 100ml of distilled water and 20ml of 10% formalin. The tissues were transferred into the second chromatin solution and left for another 2 days. After the second day, this second chromatin solution was replaced with a fresh one. The tissues were left in the fresh chromatin solution for another three days. Next, the tissues were placed in a 0.75% silver nitrate solution containing 0.75g of silver nitrate dissolved in 100 ml of distilled water and left for three days in a row; the silver nitrate solution was changed daily. Tissue pieces were placed in a petri dish and the silver deposits were gently brushed off after the tissue pieces had been impregnated for 72 hours in silver nitrate. At this point, the tissue blocks were handled extremely delicately and cautiously. The tissues underwent a 10-minute dehydration process in absolute alcohol, followed by a 30-minute paraffin infiltration and subsequent embedding in paraffin wax. A rotary microtome then sectioned the tissue blocks at 60µm. Following a 10-minute soak in 70% alcohol, the sliced pieces were placed in xylene to become translucent, mounted on gelatin-coated glass slides, coverslipped with DPX, and left to dry for four days at room temperature.
The brain samples of the experimental animals were bisected at the level of the optic chiasma. They were fixed, dehydrated, cleared, infiltrated, embedded and sectioned at 5µm. These sections were mounted on gelatin-coated slides and routinely stained with Haematoxylin and Eosin and Cresyl violet stains. The corpus callosum was measured in the midline at the level of the optic chiasma, midline. The sensorimotor cortex was quantitatively assessed by taking measures in the dorsolateral region (Femi-Akinlosotu *et al*., 2019).

Histomorphometry: Using an Olympus CH (Japan) microscope connected to TS view analysis software at x40 magnification, the dendritic arbors of the pyramidal cells were visualised for the golgi stained sections. Only the layer V pyramidal neurons were subjected to light microscopic examination. Cortical and corpus callosum thicknesses were measured in the H&E stained slides of the control and experiment groups using the measurement module of the TS view image analysis software that came with the microscope.

Cell Count Analyses: Cell count analyses were performed on the Cresyl-stained slides using an Olympus CH image microscope connected to TS view analysis software and an X40 objective lens. Only visible nuclei were used to count cells. The following common standards were used to differentiate between pyramidal and non-pyramidal neurons: (1) Pyramidal neurons displayed a distinctive triangular shape with a single large apical dendrite. (2) Non-pyramidal neurons were distinguished by their smaller size and lack of the preceding criteria. An impartial counting frame measuring 1088 square meters was employed. The sampling field was methodically moved through the cortical layer of interest until the number of different types of pyramidal cells was determined.

Statistical analysis: Data collected were expressed as means ± SD and analyzed by one-way ANOVA test using GraphPad Prism Version 6.0 (GraphPad software, San Diego, California USA). The confidence interval was computed at the 95% level, and statistical significance was set at $p<0.05$ for the null hypothesis being true by chance.

RESULTS

The study involved 197 rats, aged three weeks, in total. A kaolin suspension was injected intracisternal into 155 subjects, while 42 individuals served as controls. Twenty-seven rats died during the induction process, leaving 128 rats that made it through. A puncture to the brainstem, most likely the respiratory centre, may have killed most of the rats; some may not have recovered consciousness following anaesthesia. Only 102 experimental rats—35 for the one-week study, 36 for the two-week study, and 31 for the four-week study—were utilized in the investigation after an additional 26 died two to three days after induction. About 70.5% of the induced 3-week-old rats in this study developed hydrocephalus.

Physical observation: The hydrocephalic rats exhibited clear hydrocephalic symptoms, such as an enlarged, dome-shaped head and an unsteady gait. After a week of kaolin injection, these characteristics were visible. They often experienced varied degrees of a hunched back, bloody discharge from the eye, and an unbalanced gait (Plate 1). When being handled, a few of them displayed aggressive behaviour.

Body weight: At one, two, and four weeks after induction, the hydrocephalic rats' weights were considerably lower than those of the age-matched controls (Fig. 1).

Gross Examination of the Brain: Upon close examination, the control brains' lateral ventricles were found to have slit-like spaces that are difficult for the unaided eye to see. The three categories of hydrocephalus—mild, moderate, and severe—were caused by different degrees of ventricular dilatation in the brains of the experimental rats.

Plate 1
(A) Control rat; (B) Hydrocephalic rat. Note the hunched back and ruffled fur in the hydrocephalic rat.

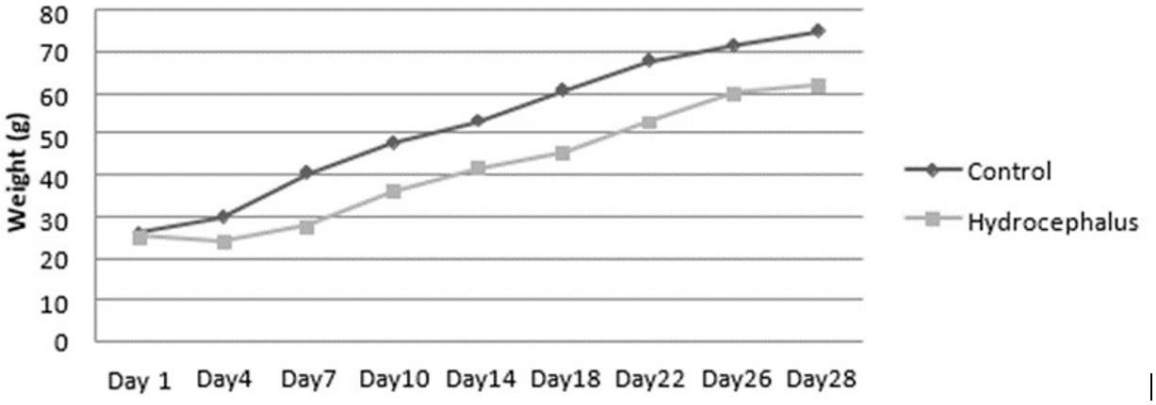

Figure 1:
Body weights of the hydrocephalic and control rats from induction until 4 weeks post-induction.

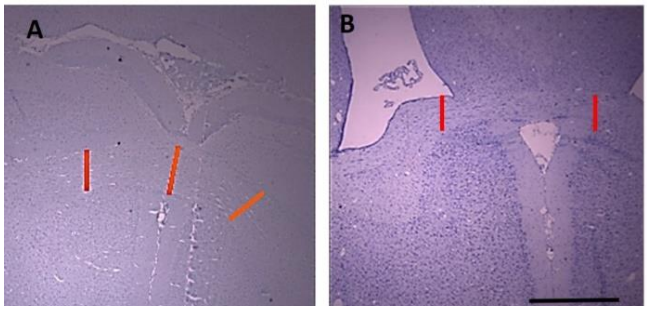

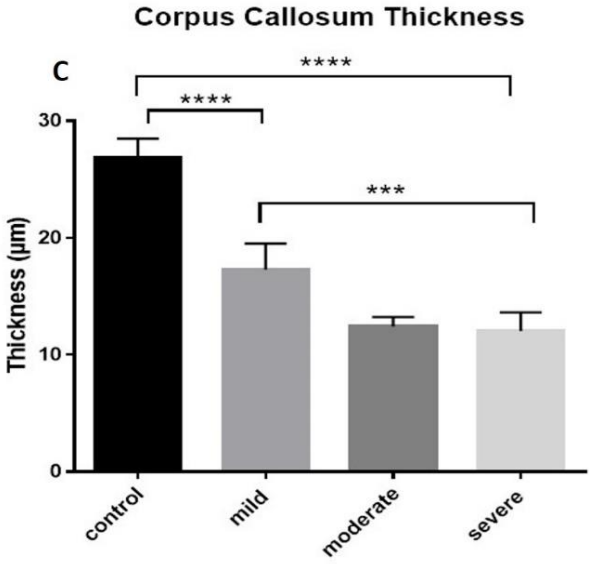

Figure 2:
(A&B) Representative cresyl violet stained brain sections of control (A) and hydrocephalic (B) rats. Note the dimensions of the corpus callosum (red line) in both control and hydrocephalic sections. Scale bar: 50µm; (C) Thickness of the corpus callosum in the various category of hydrocephalus. The corpus callosum of the control rats was significantly thicker than the hydrocephalic groups ($p<0.0001$*). The corpus callosum in mild hydrocephalic rats was significantly thicker when compared to moderate and severe hydrocephalic rats ($p=0.0064$**).

Corpus callosum thickness: Hydrocephalic rats and control groups differed significantly ($p<0.0001$) in the thickness of their corpus callosum. Compared to moderate and severe hydrocephalic rats (control: 27±0.86µm; mild: 17±1.10µm; moderate: 12±0.40µm; severe: 12±0.60µm; $p=0.0064$ respectively), the corpus callosum of mild hydrocephalic rats was significantly thicker. The thickness of the corpus callosum did not, however, differ significantly between the moderate and severe hydrocephalic rats ($p=0.2384$) (Fig. 2C).

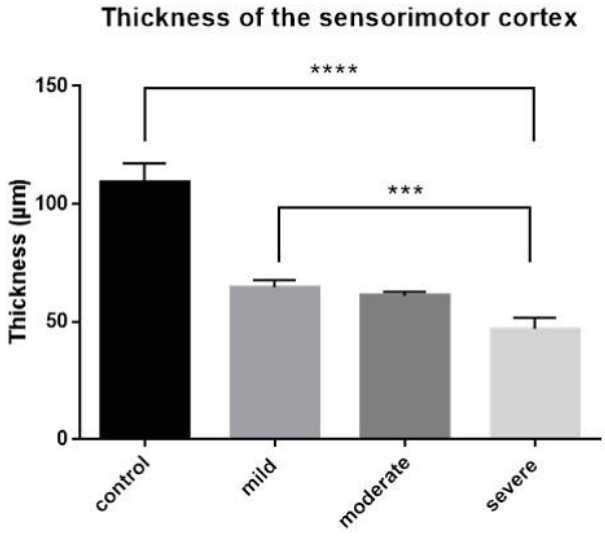

Figure 3:
Thickness of the sensorimotor cortex in the various categories of hydrocephalus. The cortex in the control rats was significantly thicker than the hydrocephalic animals ($p<0.0001$*). The cerebral cortex in mild hydrocephalic rats was significantly thicker when compared to moderate hydrocephalic rats ($p<0.05$**). The cerebral cortex in moderate hydrocephalic rats was significantly thicker when compared to severe hydrocephalic rats ($p<0.001$***).

Cortical thickness of the sensorimotor cortex: Measuring the sensorimotor cortical thickness of both control(109±3.30µm) and hydrocephalic rats (mild: 65±1.30µm; moderate: 61±0.73µm; severe: 47±1.90µm) showed a statistically significant difference ($p<0.0001$) between the control group and the various hydrocephalus categories, while there was also a significant difference ($p<0.0001$) between the various hydrocephalus categories. Rats with mild hydrocephalus had a significantly thicker cortical dimension than rats with moderate and severe hydrocephalus ($p=0.0302$ and $p<0.0001$, respectively). Rats with moderate hydrocephalus had a significantly thicker cortical dimension than those with severe hydrocephalus ($p<0.001$). (Figure 3).

Pyramidal neuron count: The pyramidal neuronal count in the hydrocephalic groups and that of their age-matched controls did not differ statistically significantly. ($p= 0.419$; 0.162; 0.791) (Table 1).

Table 1:
Pyramidal cell count in layer V of the control and hydrocephalic groups.

Group	n	Control	Hydrocephalic	p-value
1week	6	85.5±2.12	83.5±0.71	0.419
2 weeks	6	71.6± 2.88	61.7 ±6.8	0.075
4 weeks	6	86± 6.25	76 ±6.67	0.791

Golgi stain: Pyramidal cells were defined as those cells with pear-shaped cell bodies. Each soma gives rise to a single apical dendrite and a series of basal dendrites. The apical dendrite generally coursed to the cortical surface. The apical dendrites of the superficial neurons are shorter than the deeper neurons. The branching patterns of the basal dendrites in the experimental group were simple/ less complex when compared to the control groups (Plate 2).

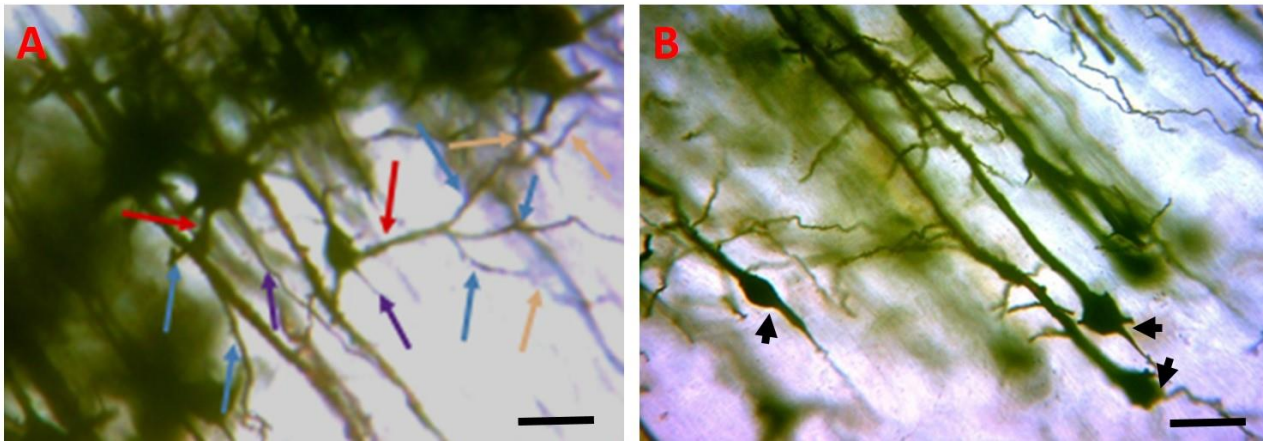

Plate 2:
Photomicrographs of Golgi-impregnated layer V pyramidal neurons of (A) control rats (2weeks post-induction) having complex branching order (basal dendrites exhibited primary, secondary and tertiary branches) compared to (B) hydrocephalic rats (2weeks post-induction) showing denudation of the basal dendrite (black arrow-heads) (red arrow: primary basal dendrite; blue arrow: secondary basal dendrite, orange arrow: tertiary dendrite; purple arrow: axon; Scale bar: 10µm).

DISCUSSION

The injection of kaolin into the cisterna magna is a well-established induction model for experimental hydrocephalus leading to inflammation and fibrosis of the CSF pathways close to the fourth ventricle apertures and in the basal subarachnoid compartment (Femi-Akinlosotu *et al*., 2019; Olopade *et al*., 2021; Chen *et al*., 2022; Parenrengi *et al*., 2024). Some rats did not develop hydrocephalus at all, while others showed varying degrees of ventriculomegaly in response to an identical volume of kaolin injected into their brains for experimentation. Extracranial lymphatic vessels have been identified as a primary pathway for the absorption of CSF. It is believed that CSF travels from the subarachnoid space via the cribriform plate, the lymphatic vessels in the olfactory submucosa, and venous system at the base of the neck (Chae *et al*., 2024; Spera *et al*., 2023). Several investigators have reported variability in ventricular distension in different animal models with internal hydrocephalus (Catalão *et al*., 2019; Czerwik *et al*., 2023) and a relationship between CSF outflow resistance (through the extra-cranial lymphatic vessels) and ventricle size in kaolin-induced hydrocephalus models (Kaolin *et al*., 2023; Nagra *et al*., 2010; Spera *et al*., 2023). Consequently, the varying degrees of ventriculomegaly might be due to the lowest lymphatic CSF absorption levels in relation to the highest degree of ventriculomegaly.

The hydrocephalic rats exhibited a hunched back, enlarged doom-shaped head, and an unsteady gait, all of which have been documented in other animal models of hydrocephalus caused by kaolin (Catalão *et al*., 2019; Femi-Akinlosotu *et al*., 2019; Chen *et al*., 2022; Kaolin *et al*., 2023; de Souza *et al*., 2024; Parenrengi *et al*., 2024). Gross examination of the induced rats' brains after sacrifice revealed varying degrees of ventriculomegaly even though some of them did not exhibit any overt symptoms of hydrocephalus.

The hydrocephalic rats showed initial weight loss and a gradual weight gain which have been reported as the earliest signs of hydrocephalus (Femi-Akinlosotu *et al*., 2019; Olopade *et al*., 2021). The hydrocephalic rats' weights were, nevertheless, consistently lower than the control groups throughout the investigation. It was also noted that the hydrocephalic rats showed little to no appetite in the first 24 to 36 hours following induction; after that, their eating patterns returned to normal. Del Bigio et. al proposed two possible explanations: either hypothalamic regulation of pituitary function might be changed, or ventricular enlargement affected the hypothalamus's centres responsible for appetite (Del Bigio *et al*., 2003). Anthropometric data from previous investigators revealed that children with hydrocephalus frequently have stunted growth, low weight, poor language, motor and social skills (Grace *et al*., 2024; Perenc *et al*., 2022; Rush *et al*., 2022) and pituitary dysfunction has been suggested as a possible cause. Fetal-onset hydrocephalus had a substantial impact on the hypothalamic gonadotrophin-releasing hormone (Catalão *et al*., 2019; McAllister *et al*., 2007). Axons in the cerebral cortex or striatum may have stretched or neurons may have disconnected, resulting in a decline in motor skills and the unsteady gait seen in hydrocephalic rats (Olopade *et al*., 2012; Chen *et al*., 2017; de Oliveira & Fabris Vidal, 2020).

The hydrocephalic rats had thinner corpus callosum, which is consistent with previous studies (Olopade *et al*., 2012; Jugé *et al*., 2016; Pozzi *et al*., 2021; Campos-Ordoñez *et al*., 2023; Rodríguez-Pérez *et al*., 2024). Stretching of the corpus callosum around the expanding ventricle results in disconnection of neurons, and atrophy of the corpus callosum is allegedly caused by a combination of mechanical injury, impaired blood flow, and accumulation of waste products in the CSF. In a hydrocephalic state, the cerebral cortex thickness indicates a state of compression (Olopade *et al*., 2012; Jugé *et al*., 2016; Campos-Ordoñez *et al*., 2023). The hydrocephalic rats and controls' pyramidal neuron counts did not vary substantially across the age ranges. This suggests that the cortex was compressed using different techniques, excluding the loss of pyramidal neurons, particularly in layer V. A decrease in the extracellular water content and venous blood flow in the impacted cortex has been suggested as the cause of the compression (Olopade *et al*., 2012; Jugé *et al*., 2016; Chen *et al*., 2017; Garcia-Bonilla *et al*., 2022; Campos-Ordoñez *et al*., 2023).

Layer V pyramidal cells, also called Betz cells, are large extra-telencephalic projection neurons that innervate α-motoneurons in the brainstem and spinal cord of primates and other mammalian species (Benavides-Piccione *et al*., 2021; Nolan *et al*., 2024). Although the hydrocephalic rats' basal dendrites primarily consist of primary basal dendrites with some denudation, the pyramidal neurons' basal dendrites in the control rats showed complex branching from primary to tertiary level. Femi-Akinlosotu et. al. noted a similar effect in day-old hydrocephalic mice (Femi-Akinlosotu *et al*., 2019). As the majority of dendritic branches form upon the arrival of thalamic fibers and other afferent fibers, the decrease in dendritic branching (basal dendrites) of pyramidal neurons may be the result of cortical de-afferentation. The basal dendrites that subcortical afferent fibers synapse on may have withdrawn or disconnected as a result of deafferentation. Alternatively, it may have been caused by the pressure of enlarged ventricles, which is first exerted on periventricular regions, affecting the basal dendrites of pyramidal neurons located deep in the cerebral cortex. The impact of hydrocephalus on the efferent axons could also be a possibility, as the trauma may impair axonal transmission by causing damage to the subcortical white matter. Because efferent connectivity to subcortical structures and the contralateral cortex is established by postnatal day 1 and predates the arrival of afferent connections, it seems unlikely that any dendritic abnormality was caused by the deafferentation of efferent axons. The direct result of the hydrocephalic process may then be the effect of hydrocephalus on the basal dendrite of pyramidal neurons, the primary efferent neurons of the cortex.

The postnatal stage of brain development is essential for the proper expression of brain-related functions (Soch *et al*., 2020; Kourosh-Arami *et al*., 2021). In terms of brain development, the 3-week-old rats used in this study are about the same age as a 6-month-old human infant (Sengupta, 2013; Zeiss, 2021). Age-related increases in brain plasticity occur as development proceeds, and developmental assaults on brain tissue can result in functional deficits. According to our research, the degree of ventriculomegaly associated with hydrocephalus altered the pyramidal neurons' basal dendrites and reduced the thickness of the cerebral cortical and corpus callosum. Although we could only qualitatively evaluate the dendritic arborization of the pyramidal neurons and there was no imaging method available to evaluate the rats' hydrocephalic status before sacrifice, we think the data from this study will serve as a foundation for future investigations into experimental hydrocephalus studies. Since neural networks are critical for survival, this research could lead to a better understanding of the circuitry configurations in the cerebral cortex and, consequently, a better understanding of the pathophysiology of juvenile hydrocephalus in experimental rats. The ultrastructure and mode of action of these synaptic connections in experimental juvenile hydrocephalic states, however, require more investigation.

Acknowledgements

The authors wish to appreciate the assistance of Mr. Oludare Osuntade, Mrs. Elizabeth Ogunsola and Mrs. Folasade Adunola for the histology slides preparation.

REFERENCES

Benavides-Piccione, R., Blazquez-Llorca, Kastanauskaite, A., Fernaud, I., Gonzalez-Tapia, S., DeFelipe, J., 2024. Key morphological features of human pyramidal neurons. bioRxiv 2023.11.10.566540. https://doi.org/10.1101/2023.11.10.566540

Benavides-Piccione, R., Rojo, C., Kastanauskaite, A., Defelipe, J., 2021. Variation in Pyramidal Cell Morphology Across the Human Anterior Temporal Lobe. *Cerebral Cortex* 31, 3592–3609. https://doi.org/10.1093/CERCOR/BHAB034

Campos-Ordoñez, T., González-Granero, S., Eudave-Patiño, M., Buriticá, J., Herranz-Pérez, V., García-Verdugo, J.M., Gonzalez-Perez, O., 2023. Normal pressure hydrocephalus decreases the proliferation of oligodendrocyte progenitor cells and the expression of CNPase and MOG proteins in the corpus callosum before behavioral deficits occur. *Exp Neurol* 365, 114412. https://doi.org/10.1016/J.EXPNEUROL.2023.114412

Catalão, C.H.R., Souza, A.O., Santos-Júnior, N.N., da Silva, S.C., da Costa, L.H.A., Alberici, L.C., Rocha, M.J.A., da Silva Lopes, L., 2019. Kaolin-induced hydrocephalus causes acetylcholinesterase activity dysfunction following hypothalamic damage in infant rats. *Brain Res* 1724, 146408. https://doi.org/10.1016/J.BRAINRES.2019.146408

Chae, J., Choi, M., Choi, J., Yoo, S.J., 2024. The nasal lymphatic route of CSF outflow: implications for neurodegenerative disease diagnosis and monitoring. *Anim Cells Syst* (Seoul) 28, 45–54. https://doi.org/10.1080/19768354.2024.2307559

Chen, L.J., Chen, J.R., Tseng, G.F., 2022. Modulation of striatal glutamatergic, dopaminergic and cholinergic neurotransmission pathways concomitant with motor disturbance in rats with kaolin-induced hydrocephalus. *Fluids Barriers CNS* 19, 1–14. https://doi.org/10.1186/S12987-022-00393-1/FIGURES/8

Chen, L.J., Wang, Y.J., Chen, J.R., Tseng, G.F., 2017. Hydrocephalus compacted cortex and hippocampus and altered their output neurons in association with spatial learning and memory deficits in rats. Brain Pathology 27, 419. https://doi.org/10.1111/BPA.12414

Curzio, D.L. Di, Curzio, D.L. Di, 2017. Neuropathological Changes in Hydrocephalus—A Comprehensive Review. *Open Journal of Modern Neurosurgery* 8, 1–29. https://doi.org/10.4236/OJMN.2018.81001

Czerwik, A., Schmidt, M.J., Olszewska, A., Hinz, S., Büttner, K., Farke, D., 2023. Reliability and interobserver variability of a grading system of ventricular distension in dogs. *Front Vet Sci* 10, 1271545. https://doi.org/10.3389/FVETS.2023.1271545/BIBTEX

de Oliveira, G.R., Fabris Vidal, M., 2020. A normal motor development in congenital hydrocephalus after Cuevas Medek Exercises as early intervention: A case report. *Clin Case Rep* 8, 1226–1229. https://doi.org/10.1002/CCR3.2860

de Souza, S.N.F., Machado, H.R., da Silva Lopes, L., da Silva Beggiora Marques, P., da Silva, S.C., Dutra, M., Aragon, D.C., Santos, M.V., 2024. Evaluation of the behavioral, histopathological, and immunohistochemical effects resulting from ventriculosubcutaneous shunt obstruction in kaolin-induced hydrocephalus in rats. *Child's Nervous System* 40, 1533–1539. https://doi.org/10.1007/S00381-023-06260-0/METRICS

Del Bigio, M.R., 2010. Neuropathology and structural changes in hydrocephalus. *Dev Disabil Res Rev* 16, 16–22. https://doi.org/10.1002/DDRR.94

Del Bigio, M.R., Wilson, M.J., Enno, T., 2003. Chronic hydrocephalus in rats and humans: White matter loss and behavior changes. *Ann Neurol* 53, 337–346. https://doi.org/10.1002/ANA.10453

Femi-Akinlosotu, O.M., Shokunbi, M.T., Naicker, T., 2019. Dendritic and synaptic degeneration in pyramidal neurons of the sensorimotor cortex in neonatal mice with kaolin-induced hydrocephalus. *Front Neuroanat* 13, 426791. https://doi.org/10.3389/FNANA.2019.00038/BIBTEX

Galakhova, A.A., Hunt, S., Wilbers, R., Heyer, D.B., de Kock, C.P.J., Mansvelder, H.D., Goriounova, N.A., 2022. Evolution of cortical neurons supporting human cognition. *Trends Cogn Sci* 26, 909–922. https://doi.org/10.1016/J.TICS.2022.08.012

Garcia-Bonilla, M., Castaneyra-Ruiz, L., Zwick, S., Talcott, M., Otun, A., Isaacs, A.M., Morales, D.M., Limbrick, D.D., McAllister, J.P., 2022. Acquired hydrocephalus is associated with neuroinflammation, progenitor loss, and cellular changes in the subventricular zone and periventricular white matter. *Fluids Barriers CNS* 19, 1–18. https://doi.org/10.1186/S12987-022-00313-3/FIGURES/7

Grace, N., Mbabazi, E., Mukunya, D., Tumuhamye, J., Okechi, H., Wegoye, E., Olupot-Olupot, P., Matovu, J.K., Hopp, L., Napyo, A., 2024. High burden of wasting among children under-five with hydrocephalus receiving care at CURE children's hospital in Uganda: a cross-sectional study. *BMC Nutr* 10, 1–10. https://doi.org/10.1186/S40795-024-00819-Z/TABLES/2

Hunt, S., Leibner, Y., Mertens, E.J., Barros-Zulaica, N., Kanari, L., Heistek, T.S., Karnani, M.M., Aardse, R., Wilbers, R., Heyer, D.B., Goriounova, N.A., Verhoog, M.B., Testa-Silva, G., Obermayer, J., Versluis, T., Benavides-Piccione, R., De Witt-Hamer, P., Idema, S., Noske, D.P., Baayen, J.C., Lein, E.S., Defelipe, J., Markram, H., Mansvelder, H.D., Schürmann, F., Segev, I., De Kock, C.P.J., 2023. Strong and reliable synaptic communication between pyramidal neurons in adult human cerebral cortex. *Cerebral Cortex* 33, 2857–2878. https://doi.org/10.1093/CERCOR/BHAC246

Jugé, L., Pong, A.C., Bongers, A., Sinkus, R., Bilston, L.E., Cheng, S., 2016. Changes in Rat Brain Tissue Microstructure and Stiffness during the Development of Experimental Obstructive Hydrocephalus. *PLoS One* 11, e0148652. https://doi.org/10.1371/JOURNAL.PONE.0148652

Kahle, K.T., Klinge, P.M., Koschnitzky, J.E., Kulkarni, A. V., MacAulay, N., Robinson, S., Schiff, S.J., Strahle, J.M., 2024. Paediatric hydrocephalus. *Nature Reviews Disease Primers* 2024 10:1 10, 1–16. https://doi.org/10.1038/s41572-024-00519-9

Kahle, K.T., Kulkarni, A. V., Limbrick, D.D., Warf, B.C., 2016. Hydrocephalus in children. *The Lancet* 387, 788–799. https://doi.org/10.1016/S0140-6736(15)60694-8

Kaolin, D., Kan, O., Ile, E., Hidrosefali, İ., Aquaporin, Ü., İntrakraniyal, E., Ölçümü, B., Hayvan, A.:, Elif, D., Gündoğdu, B., Aydin, H.E., Avci Küpeli, Z., 2023. Intracranial Pressure Measurement of and Investigation of the Effect of Aquaporin on Hydrocephalus Induced by Experimental Kaolin and Autologous Blood Injection: An Animal Study. Turkiye Klinikleri *J Med Sci* 43, 149–59. https://doi.org/10.5336/medsci.2022-93849

Kourosh-Arami, M., Hosseini, N., Komaki, A., 2021. Brain is modulated by neuronal plasticity during postnatal development. Journal of Physiological Sciences 71, 1–16. https://doi.org/10.1186/S12576-021-00819-9/TABLES/1

Maller, V. V., Gray, R.I., 2016. Noncommunicating Hydrocephalus. Seminars in Ultrasound, CT and MRI 37, 109–119. https://doi.org/10.1053/J.SULT.2015.12.004

McAllister, J.P., Abdolvahabi, R.M., Walker, M.L., Mitchell, J.A., Jones, H.C., 2007. Effects of congenital hydrocephalus on the hypothalamic gonadotrophin-releasing hormone system. *Neurosurg Focus* 22, 1–10. https://doi.org/10.3171/FOC.2007.22.4.5

Nagra, G., Wagshul, M.E., Rashid, S., Li, J., McAllister, J.P., Johnston, M., 2010. Elevated CSF outflow resistance associated with impaired lymphatic CSF absorption in a rat model of kaolin-induced communicating hydrocephalus. *Cerebrospinal Fluid Res* 7, 4. https://doi.org/10.1186/1743-8454-7-4

Nolan, M., Scott, C., Hof, P.R., Ansorge, O., 2024a. Betz cells of the primary motor cortex. *J Comp Neurol* 532, 1–29. https://doi.org/10.1002/CNE.25567

Nolan, M., Scott, C., Hof, P.R., Ansorge, O., 2024b. Betz cells of the primary motor cortex. *J Comp Neurol* 532, 1–29. https://doi.org/10.1002/CNE.25567

Olopade, F.E., Femi-Akinlosotu, O., Adekanmbi, A.J., Ajani, S., Shokunbi, M.T., 2021. Neurobehavioural changes and morphological study of cerebellar purkinje cells in kaolin induced hydrocephalus. *Anat Sci Int* 96, 87–96. https://doi.org/10.1007/S12565-020-00561-Z/METRICS

Olopade, F.E., Shokunbi, M.T., Sirén, A.L., 2012. The relationship between ventricular dilatation, neuropathological and neurobehavioural changes in hydrocephalic rats. *Fluids Barriers CNS* 9, 19. https://doi.org/10.1186/2045-8118-9-19

Parenrengi, M.A., Dariansyah, A.D., Suryaningtyas, W., Fauziah, D., Sudiana, I.K., Utomo, B., Gunawan, P.I., 2024. Effects of Cerebrospinal Fluid Drainage on Pro-Inflammatory and Anti-Inflammatory Cytokines Expression in the Subventricular Zone of Kaolin-Induced Hydrocephalic Rats. *Pharmacognosy Journal* 16, 20–27. https://doi.org/10.5530/pj.2024.16.3

Perenc, L., Guzik, A., Podgórska-Bednarz, J., Drużbicki, M., 2022. Somatic Development Disorders in Children and Adolescents Affected by Syndromes and Diseases Associated with Neurodysfunction and Hydrocephalus Treated/Untreated Surgically. *International Journal of Environmental Research and Public Health* 2022, Vol. 19, Page 5712 19, 5712. https://doi.org/10.3390/IJERPH19095712

Pozzi, N.G., Brumberg, J., Todisco, M., Minafra, B., Zangaglia, R., Bossert, I., Trifirò, G., Ceravolo, R., Vitali, P., Isaias, I.U., Fasano, A., Pacchetti, C., 2021. Striatal Dopamine Deficit and Motor Impairment in Idiopathic Normal Pressure Hydrocephalus. *Movement Disorders* 36, 124–132. https://doi.org/10.1002/MDS.28366

Rekate, H.L., Blitz, A.M., 2016. Hydrocephalus in children. Handb *Clin Neurol* 136, 1261–1273. https://doi.org/10.1016/B978-0-444-53486-6.00064-8

Rodríguez-Pérez, L.M., López-de-San-Sebastián, J., de Diego, I., Smith, A., Roales-Buján, R., Jiménez, A.J., Paez-Gonzalez, P., 2024. A selective defect in the glial wedge as part of the neuroepithelium disruption in hydrocephalus development in the mouse hyh model is associated with complete corpus callosum dysgenesis. *Front Cell Neurosci* 18, 1330412. https://doi.org/10.3389/FNCEL.2024.1330412/BIBTEX

Rush, J., Paľa, A., Kapapa, T., Wirtz, C.R., Mayer, B., Micah-Bonongwe, A., Gladstone, M., Kamalo, P., 2022. Assessing neurodevelopmental outcome in children with hydrocephalus in Malawi. A pilot study. Clin *Neurol Neurosurg* 212, 107091. https://doi.org/10.1016/J.CLINEURO.2021.107091

Sarkala, H.B., Jahanshahi, M., Dolatabadi, L.K., Namavar, M.R., 2023. G-CSF improved the memory and dendritic

morphology impairments in the hippocampal CA1 pyramidal neurons after brain ischemia in the male rats. *Metab Brain Dis* 38, 2573–2581. https://doi.org/10.1007/S11011-023-01286-4/METRICS

Sengupta, P., 2013. The Laboratory Rat: Relating Its Age with Human's. *Int J Prev Med* 4, 624.

Soch, A., Sominsky, L., Younesi, S., De Luca, S.N., Gunasekara, M., Bozinovski, S., Spencer, S.J., 2020. The role of microglia in the second and third postnatal weeks of life in rat hippocampal development and memory. Brain Behav Immun 88, 675–687. https://doi.org/10.1016/J.BBI.2020.04.082

Spera, I., Cousin, N., Ries, M., Kedracka, A., Castillo, A., Aleandri, S., Vladymyrov, M., Mapunda, J.A., Engelhardt, B., Luciani, P., Detmar, M., Proulx, S.T., 2023. Open pathways for cerebrospinal fluid outflow at the cribriform plate along the olfactory nerves. *EBioMedicine* 91. https://doi.org/10.1016/J.EBIOM.2023.104558

Suryaningtyas, W., Arifin, M., Rantam, F.A., Bajamal, A.H., Dahlan, Y.P., Dewa Gede Ugrasena, I., Maliawan, S., 2019. Erythropoietin protects the subventricular zone and inhibits reactive astrogliosis in kaolin-induced hydrocephalic rats. Child's Nervous System 35, 469–476. https://doi.org/10.1007/S00381-019-04063-W/METRICS

Zeiss, C.J., 2021. Comparative Milestones in Rodent and Human Postnatal Central Nervous System Development. *Toxicol Pathol* 49, 1368–1373. https://doi.org/10.1177/01926233211046933/ASSET/IMAGES/LARGE/10.1177_01926233211046933-FIG1.JPEG